MagnetoSperm: A microrobot that navigates using weak magnetic fields

Islam S. M. Khalil,[1,a)] Herman C. Dijkslag,[2] Leon Abelmann,[3,4] and Sarthak Misra[2,b)]
[1]*German University in Cairo, New Cairo City 13411, Egypt*
[2]*MIRA–Institute for Biomedical Technology and Technical Medicine, University of Twente, 7500 AE Enschede, The Netherlands*
[3]*MESA+ Institute for Nanotechnology, University of Twente, 7500 AE Enschede, The Netherlands*
[4]*Korean Institute of Science and Technology, 66123 Saarbrücken, Germany*

(Received 19 January 2014; accepted 20 March 2014; published online 2 June 2014)

In this work, a propulsion system similar in motion to a sperm-cell is investigated. This system consists of a structure resembling a sperm-cell with a magnetic head and a flexible tail of 42 μm and 280 μm in length, respectively. The thickness, length, and width of this structure are 5.2 μm, 322 μm, and 42 μm, respectively. The magnetic head includes a 200 nm-thick cobalt-nickel layer. The cobalt-nickel layer provides a dipole moment and allows the flexible structure to align along oscillating weak (less than 5 mT) magnetic field lines, and hence generates a propulsion thrust force that overcomes the drag force. The frequency response of this system shows that the propulsion mechanism allows for swimming at an average speed of 158 $\pm$ 32 μm/s at alternating weak magnetic field of 45 Hz. In addition, we experimentally demonstrate controlled steering of the flexible structure towards reference positions. © *2014 AIP Publishing LLC*. [http://dx.doi.org/10.1063/1.4880035]

Electromagnetic systems and magnetic microrobots have become an active area of study because of their potential to carry-out limited non-trivial tasks.[1–4] However, the limited projection distance of the magnetic field gradients generated using electromagnetic systems has motivated many researchers[5–14] to investigate several propulsion mechanism and use electromagnetic coils only for steering. Dreyfus *et al.*[11] and Zhang *et al.*[5] have developed microrobots with flexible longitudinal and rigid helical structures that move using oscillating and rotating magnetic fields, respectively. These structures were inspired by the natural design of the sperm-flagella and the *E. coli* bacteria. Gillies *et al.*[15] have modeled the sperm flagellar motion in a microscopic slide chamber to obtain the flagellar beat frequency and head centroid position. Tony *et al.* have also investigated the propulsion mechanism of a macroscopic swimmer (with flagellar motion) through measurements of propulsive forces and time-varying shapes.[16] However, properties of this propulsion mechanism (e.g., the frequency response and motion control techniques) at microscale has not yet been shown.

In this study, we discuss the properties and characterization of a self-propelled microrobot which we refer to as MagnetoSperm. This microrobot is similar in shape to a sperm-cell. It can be steered and propelled using weak oscillating magnetic fields. These fields would allow the flexible structure of MagnetoSperm to oscillate and generate a thrust force, as shown in Fig. 1. (*Please refer to the accompanying video that demonstrates the propulsion of MagnetoSperm using oscillating weak magnetic fields.*) We characterize the frequency response of MagnetoSperm using an oscillating field with a frequency range of 0 Hz–65 Hz (the beat frequency of a flagellum of a sperm cell ranges from 20 Hz to 50 Hz).[17] This characterization is used to determine the maximum swimming speed that can be used in the design of a feedback control system for the motion of MagnetoSperm.

MagnetoSperm consists of an ellipsoid head and a trapezoidal tail to mimic the shape of a sperm-cell. Fabrication of MagnetoSperm is done essentially in two steps (Fig. 2). First, the head, neck, and tail structures are defined from an SU-8 polymer using photolithography. SU-8 has been chosen for its mechanical stability and ease of fabrication. Second, a 200 nm thick cobalt-nickel layer ($Co_{80}Ni_{20}$) is patterned on the head by lift-off.

The propulsion of MagnetoSperm is provided by the oscillating weak magnetic fields that exerts a magnetic torque on the magnetic dipole of ellipsoid head. We calculate the drag force and the magnetic force on MagnetoSperm to show that it swims using the weak oscillating fields rather

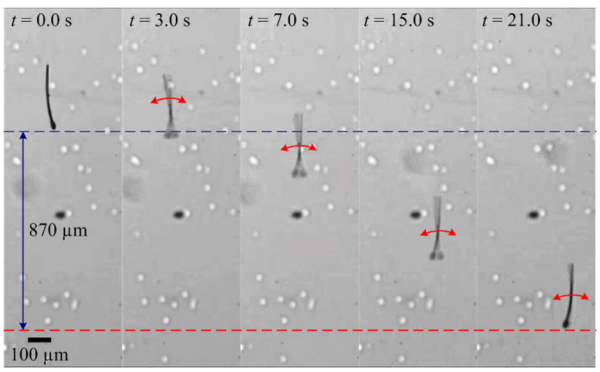

FIG. 1. MagnetoSperm moving under the influence of the oscillating (25 Hz) weak magnetic fields (~5 mT). At $t = 0$ s, zero magnetic field is applied. At $t = 1$ s, oscillating weak magnetic fields are applied. The magnetic torque exerted on the dipole moment of MagnetoSperm oscillates its flexible tail and results in a thrust force. This thrust force allows MagnetoSperm to swim at a speed of 53 μm/s. The dashed blue and red lines indicate the starting and ending positions of MagnetoSperm. *Please refer to the accompanying video that demonstrates the propulsion of MagnetoSperm using oscillating weak magnetic fields.* (Multimedia view) [URL: http://dx.doi.org/10.1063/1.4880035.1]

a)Electronic mail: islam.shoukry@guc.edu.eg.
b)Electronic mail: s.misra@utwente.nl.

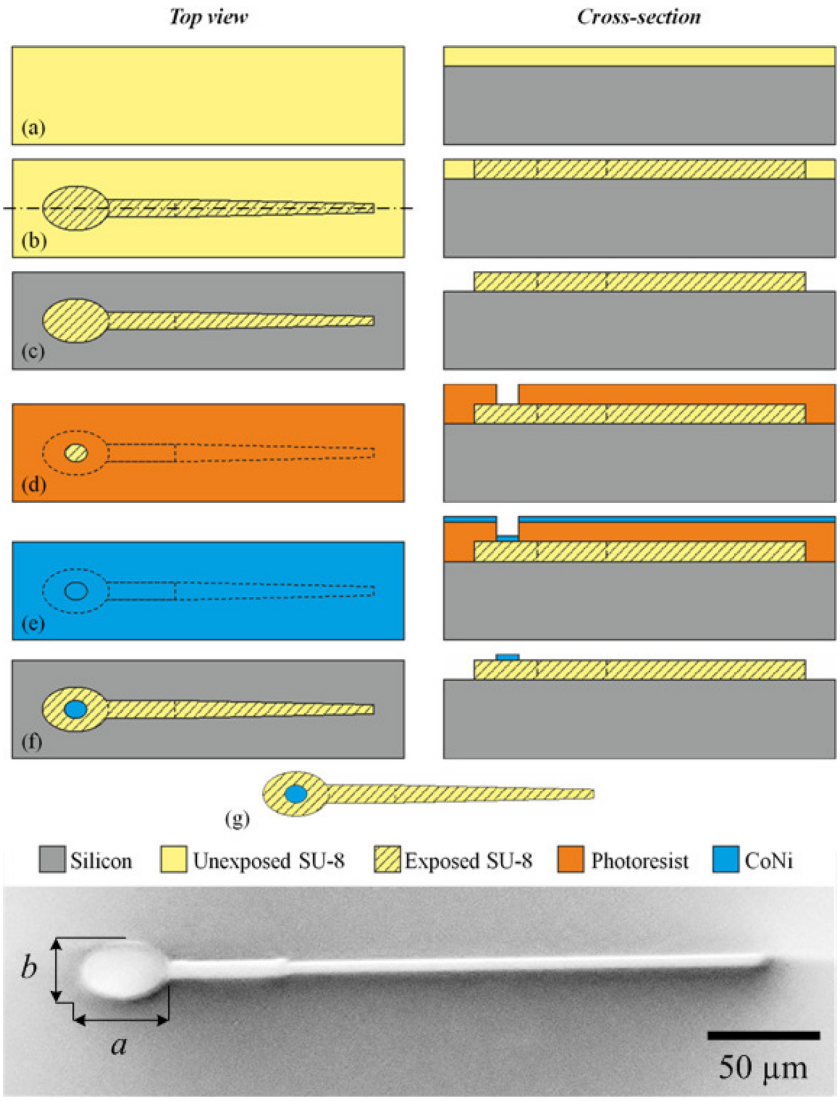

FIG. 2. Schematic illustration of the fabrication of MagnetoSperm: A 5 μm SU-8 layer is spin-coated on a silicon support wafer (a) and patterned using standard photolithography ((b), (c)). Using a resist lift-off mask (d), a 200 nm $Co_{80}Ni_{20}$ element is defined on the head by e-beam evaporation ((d), (e)). The MagnetoSperm is released into liquid by etching the entire silicon wafer in a 5% tetramethylammonium hydroxide solution at 85 °C. The major and minor diameters of the ellipsoid head of MagnetoSperm are indicated by a (42.6 μm) and b (27.6 μm), respectively.

than the magnetic field gradients. A lower limit of the drag force on MagnetoSperm can be obtained by neglecting its head and assuming that its morphology is similar to a long thin needle of length (l) and diameter (d)[18]

$$\mathbf{F_d}(\dot{\mathbf{P}}) = \eta \frac{l}{\ln\left(\frac{2l}{d}\right) - 0.81}\dot{\mathbf{P}}, \tag{1}$$

where $\mathbf{F_d}(\dot{\mathbf{P}})$ and $\dot{\mathbf{P}}$ are the drag force and the velocity of MagnetoSperm, respectively. Further, η is the dynamic viscosity of water (1 mPa s), and l and d are the length (322 μm) and diameter (5.2 μm) of MagnetoSperm, respectively. Using (1), the linear drag force is calculated to be 1.2×10^{-11} N at a speed of 158 μm/s (maximum average speed of MagnetoSperm at frequency of 45 Hz). The magnetic force exerted on the magnetic dipole of MagnetoSperm is given by

$$\mathbf{F}(\mathbf{P}) = \int_v M_s \mathrm{d}v \cdot \nabla \mathbf{B}(\mathbf{P}) = \mathbf{m} \cdot \nabla \mathbf{B}(\mathbf{P}), \tag{2}$$

where $\mathbf{F}(\mathbf{P})$ is the magnetic force at point ($\mathbf{P}$). Further, M_s and v are the magnetization saturation (1.19×10^6 A/m) and volume of the $Co_{80}Ni_{20}$ that is deposited on the head of MagnetoSperm, respectively. Further, $\mathbf{B}(\mathbf{P})$ is the magnetic field at point ($\mathbf{P}$). Using (2), the maximum magnetic force exerted on MagnetoSperm is calculated to be 3.89×10^{-13} N at magnetic field gradient of 2 mT/m. This calculation shows that the maximum magnetic force exerted on the MagnetoSperm by our magnetic system is 2 orders-of-magnitude smaller than the drag force. Therefore, motion of MagnetoSperm (Fig. 1) is due to the thrust force generated based on the oscillation of the flexible tail. This result would allow us to propel (Fig. 1) and steer (Fig. 4) MagnetoSperm using weak magnetic fields without the magnetic field gradients.

We use an electromagnetic system to provide uniform weak magnetic fields to move and steer MagnetoSperm. The field lines are oscillated to move MagnetoSperm in two-dimensional space. The angle between the oscillating magnetic field lines is approximately 90°. Position of MagnetoSperm is detected using a microscopic system and a feature tracking algorithm.[19] Uniform magnetic fields are applied and oscillated with a frequency range of 0 Hz–65 Hz. This frequency range is devised based on the frequency response of our electromagnetic coils. The

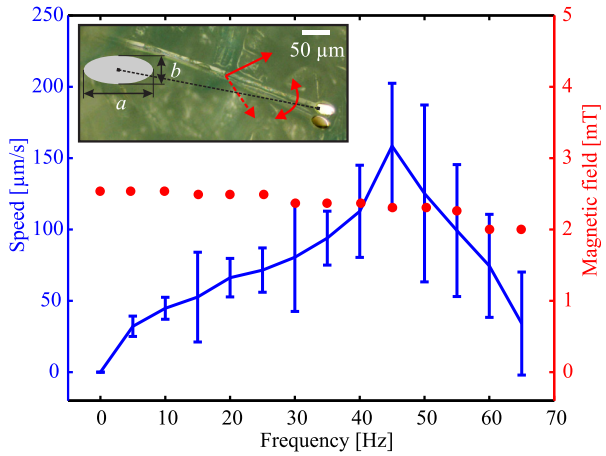

FIG. 3. Frequency response of MagnetoSperm (upper-left corner) and single air-core electromagnetic coil. Average speed of MagnetoSperm and magnitude of magnetic fields are calculated from 5 trials and measurements at each frequency, respectively. Magnetic fields are measured using a calibrated three-axis Hall magnetometer (Sentron AG, Digital Teslameter 3MS1-A2D3-2-2 T, Switzerland). The average speed decreases at oscillating magnetic field with frequency of 50 Hz. The red arrows represent the oscillating magnetic fields with an angle of approximately 90°. The major and minor diameters of the ellipsoid head of MagnetoSperm are indicated by a (42.6 μm) and b (27.6 μm), respectively. *Please refer to the accompanying video that shows a simulation of the oscillating magnetic fields.* (Multimedia view) [URL: http://dx.doi.org/10.1063/1.4880035.1]

magnitude of the magnetic field drops by 50% at approximately 80 Hz (50% of the magnetic field magnitude at 0 Hz).

The magnitude of the magnetic fields within the frequency range of 0 Hz–65 Hz is almost constant (Fig. 3). The slight decrease of the magnitude of the magnetic fields has a negligible effect on the oscillation of MagnetoSperm as a low magnitude of torque will ultimately align the MagnetoSperm along the field lines. However, the oscillation amplitude of MagnetoSperm decreases as we increase the frequency of the oscillating magnetic fields. Therefore, the change in the swimming velocity is only due to the frequency of the oscillating fields that controls the oscillation amplitude of MagnetoSperm. Fig. 3 shows that increasing the frequency of the oscillating fields above 45 Hz results in a decrease in the swimming speed. We attribute this decrease to the oscillation amplitude that decreases at high frequencies since MagnetoSperm can no longer follow the oscillating field lines.

We measure the average speed at each frequency 5 times. Fig. 3 shows the frequency response of MagnetoSperm in the mentioned frequency range. We observe that the maximum swimming speed is 158 ± 32 μm/s at alternating weak magnetic field (less than 5 mT) of 45 Hz. Increasing the frequency of the oscillating fields more than 45 Hz results in a decrease in the average swimming speed of MagnetoSperm.

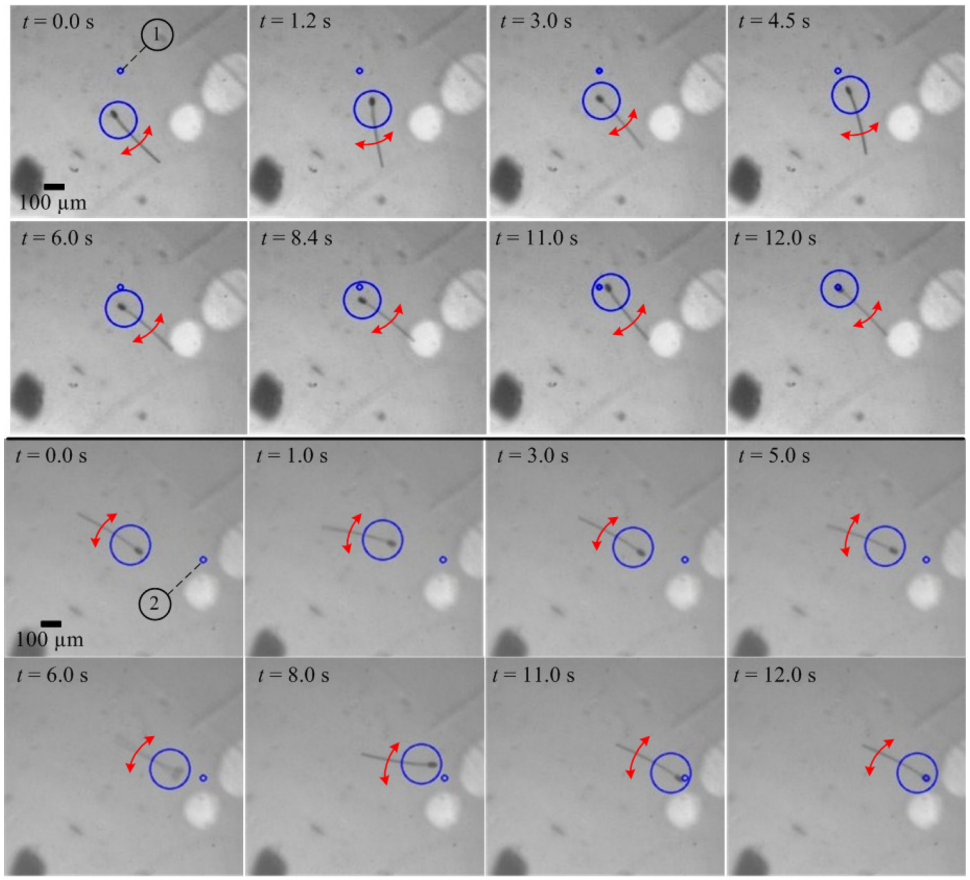

FIG. 4. MagnetoSperm is steered towards two reference positions (small blue circles) under the influence of the controlled oscillating magnetic fields of 5 Hz. The oscillating magnetic fields are directed towards the reference position to move and steer MagnetoSperm. The red arrow indicates the oscillation of the MagnetoSperm, whereas the large blue circle is assigned using a feature tracking algorithm.[14] *Please refer to the accompanying video that demonstrates the steering and propulsion of MagnetoSperm using oscillating weak magnetic fields.* (Multimedia view) [URL: http://dx.doi.org/10.1063/1.4880035.1]

Fig. 3 shows a qualitative match of the maximum swimming speed between our experimental results and those measured by Dreyfus *et al.*[11] The difference between the maximum swimming speed is due to the size, morphology, properties of medium that affect the beating frequency of the tail, and hence affect the swimming speed of the structure.[20]

The frequency response of MagnetoSperm can be used to control its swimming speed during a point-to-point motion control task. This can be done by directing the magnetic field lines towards a reference position and oscillating the fields to induce a thrust force through the flexible tail. Fig. 4 shows the motion of MagnetoSperm at a frequency of 5 Hz. In this representative experiment, the magnetic fields are oriented towards two reference positions (small blue circle). The magnetic dipole moment of MagnetoSperm allows for its alignment along the field lines. Motion of MagnetoSperm is observed after the oscillation of the applied field lines. *Please refer to the accompanying video that demonstrates the steering and propulsion of MagnetoSperm using oscillating weak magnetic fields*.

In conclusion, we present a microscopic investigation on a propulsion mechanism using oscillating weak magnetic fields. This investigation includes the manufacturing and characterization of MagnetoSperm which consists of a magnetic head and a flexible tail. The frequency response characterization shows that MagnetoSperm swims at average speed of 0.1 body lengths per second to 0.5 body lengths per second for a frequency range of 5 Hz–45 Hz.

The research leading to these results has received funding from MIRA-Institute for Biomedical Technology and Technical Medicine, University of Twente. The authors thank Ms. Ozlem Sardan Sukas for assistance with the design and manufacturing of the MagnetoSperm.

[1]B. J. Nelson, I. K. Kaliakatsos, and J. J. Abbott, Annu. Rev. Biomed. Eng. **12**, 55–85 (2010).
[2]J. Wang and W. Gao, ACS Nano **6**, 5745–5751 (2012).
[3]M. P. Kummer, J. J. Abbott, B. E. Kartochvil, R. Borer, A. Sengul, and B. J. Nelson, IEEE Trans. Rob. **26**, 1006–1017 (2010).
[4]S. Sanchez, A. A. Solovev, S. Schulze, and O. G. Schmidt, Chem. Commun. **47**, 698–700 (2011).
[5]L. Zhang, J. J. Abbott, L. Dong, B. E. Kratochvil, D. Bell, and B. J. Nelson, Appl. Phys. Lett. **94**, 064107 (2009).
[6]W. F. Paxton, K. C. Kistler, C. C. Olmeda, A. Sen, S. K. S. Angelo, Y. Cao, T. E. Mallouk, P. E. Lammert, and V. H. Crespi, J. Am. Chem. Soc. **126**, 13424–13431 (2004).
[7]S. Fournier-Bidoz, A. C. Arsenault, I. Manners, and G. A. Ozin, Chem. Commun. **2005**, 441–443.
[8]J. R. Howse, A. J. Ryan, T. Gough, R. Vafabakhsh, and R. Golestanian, Phys. Rev. Lett. **99**, 048102 (2007).
[9]Y. F. Mei, A. A. Solovev, S. Sanchez, and O. G. Schmidt, Chem. Soc. Rev. **40**, 2109–2119 (2011).
[10]S. Sanchez, A. A. Solovev, S. M. Harazim, and O. G. Schmidt, J. Am. Chem. Soc. **133**, 701–703 (2011).
[11]R. Dreyfus, J. Baudry, M. L. Roper, M. Fermigier, H. A. Stone, and J. Bibette, Nature **437**, 862–865 (2005).
[12]A. A. Solovev, S. Sanchez, M. Pumera, Y. F. Mei, and O. G. Schmidt, Adv. Funct. Mater. **20**, 2430–2435 (2010).
[13]J. G. Gibbs and Y.-P. Zhao, Appl. Phys. Lett. **94**, 163104 (2009).
[14]I. S. M. Khalil, V. Magdanz, S. Sanchez, O. G. Schmidt, and S. Misra, Appl. Phys. Lett. **103**, 172404 (2013).
[15]E. Gillies, R. Cannon, R. Green, and A. Pacey, J. Fluid Mech. **625**, 445 (2009).
[16]E. L. Tony, S. Yu, and A. E. Hosoi, Phys. Fluids **18**, 091701 (2006).
[17]E. Lauga and T. Powers, Rep. Prog. Phys. **72**, 096601 (2009).
[18]T. J. Ui, R. G. Hussey, and R. P. Roger, Phys. Fluids **27**, 787 (1984).
[19]I. S. M. Khalil, V. Magdanz, S. Sanchez, O. G. Schmidt, and S. Misra, IEEE Trans. Rob. **30**, 49–58 (2013).
[20]M. Gomendio, A. F. Malo, J. Garde, and E. R. S. Roldan, Reproduction **134**, 19–29 (2007).